From Spill to Sequestration: The Molecular Journey of Contamination via Comprehensive Multiphase NMR

Hussain Masoom[1], Denis Courtier-Murias[1], Ronald Soong[1], Werner E. Maas[2], Michael Fey[2], Rajeev Kumar[3], Martine Monette[3], Henry J. Stronks[3], Myrna J. Simpson[1], and André J. Simpson[1*]

1. Department of Chemistry, University of Toronto, Toronto, ON, Canada, M1C 1A4
2. Bruker BioSpin Corp., Billerica, Massachusetts, USA, 01821-3991
3. Bruker BioSpin Canada, Milton, ON, Canada, L9T 1Y6

This supplementary information contains 15 pages, 3 figures and 1 table.

***Corresponding Author Information:**

André J. Simpson

Department of Chemistry

University of Toronto Scarborough

1265 Military Trail

Toronto, Ontario.

Canada, M1C 1A4

Telephone: 1+(416)-287-7547

Fax : 1+(416)-287-7279

Email: andre.simpson@utoronto.ca

SUPPLEMENTARY INFORMATION

S.1 Experimental Instrument Methods

Spectral Editing

Diffusion-edited ^{19}F and spectra were collected using a bipolar pulse pair longitudinal encode−decode (BPLED) sequence with inverse gated decoupling.[1] Scans were collected using encoding/decoding gradients of 1.2ms at 50 gauss/cm and a diffusion time of 100ms. Inverse diffusion edited (IDE) and recovering relaxation losses arising from diffusion editing (RADE) were created via difference from the appropriate controls as previously described.[2]

Kinetics Experiments

Solution state (inverse diffusion editing) and gel phase (diffusion editing) experiments used spectral editing techniques described elsewhere.[2] Considering the relatively low sensitivity of the experiments the intensity was refocused into a single spike which greatly improves signal-to-noise for detection. This technique is called CPMG single spike (CPMG-SS) described elsewhere,[3] and permits the kinetic experiments to be repeated more rapidly providing higher temporal resolution. The drawback is loss of chemical shift information, but this is not an issue if the goal is simply to monitor the quantity of contaminant in each phase over time. Kel-F caps and Kel-F seals had to be used to seal the liquids in the study. The seals were placed as high as physically possible to ensure they were not directly in the coil region however, background was not always completely cancelled by the phase cycles in the single spike experiments. As such

blanks were run (an identical rotor without ^{19}F contaminant) and subtracted to give just the single spike signal from the contaminant itself by difference.

1D ^{19}F solution and gel phase CPMG-SS experiments were performed with 16 scans, 8 dummy scans, a recycle delay of 5 x T_1, and 4096 time domain points. A 7µs 44W pulse was used for echo formation with 988 loops and a delay of 12µs. Spectra were zero filled by a factor of 2 and processed using an exponential function corresponding to a line broadening of 10 Hz in the final spectrum.

Solid state ^{19}F-^{13}C CP CPMG-SS experiments for kinetic curves were performed with a 80-100% ramp, a contact time of 2.5ms, and high power composite pulse decoupling (Spinal-64). The number of scans were 320 with 8 dummy scans, a recycle delay of 5 x T_1 and 1024 time domain points. A 15µs 6W pulse was used for echo formation with 250 loops and a delay of 18µs. The power of the CPMG train was reduced to protect the NMR probe as both high power decoupling and the CMPG train had to be applied simultaneously. Spectra were zero filled by a factor of 2 and processed using an exponential function corresponding to a line broadening of 50Hz in the final spectrum.

Experiments for Molecular Interactions

Solid state ^{1}H-^{19}F CP experiments for the CP build up curves were performed with a linear ramp defined by 100 points ranging from 80-100% of the full contact power. The contact time was arrayed from 0.05-5ms and high power composite pulse decoupling (Spinal-64) applied during acquisition. The number of scans was 8192 with 16 dummy scans, a recycle delay of 5 x T_1 and 2048 time domain points. Spectra were zero filled by a factor of 2 and processed

using an exponential function corresponding to a line broadening of 50 Hz in the final spectrum. Build up curves were plotted and analyzed using SigmaPlot (Version 11, Systat Software, Inc. Germany).

Solid state ^{19}F-^{1}H CP experiments were performed using a modified CP experiment with ^{1}H pre-saturation added for suppression of the residual water signal. An 80-100% ramp was used with a contact time from 2 ms. The number of scans was 28672 with 16 dummy scans, a recycle delay of 5 x T_1 and 2048 time domain points. Spectra were zero filled by a factor of 2 and processed using an exponential function corresponding to a line broadening of 50 Hz in the final spectrum.

^{1}H-^{19}F observe Heteronuclear Saturation Transfer Difference (HSTD) experiments were performed with an NMR experiment similar to the one described in Longstaffe et al.[4] 138240 scans were used for PFOA and 77824 scans for PFP were acquired with 128 dummy scans, 16384 time domain points, and a recycle delay of 5 x T_1. 0.05W of saturation power was delivered to all ^{1}H nuclei by scanning the full range of ^{1}H resonances from +200 to +4000Hz in 200Hz increments. Off resonance pulses were +1000000 Hz away. For PFP, a T_2 filter was used to isolate gel phase interactions because signal from semi-rigid peaks complicated quantification. The T_2 filter employed 32 loops with a delay of 150µs between each loop and optimized empirically to suppress the rigid components only. Spectra were zero filled by a factor of 2 and processed using an exponential function corresponding to a line broadening of 10Hz in the final spectrum. Reference spectra were acquired with the same conditions except with 16 scans for PFOA and 512 scans for PFP both with 8 dummy scans.

^{19}F-^{1}H Reverse Heteronuclear Saturation Transfer Difference (RHSTD) was performed as previously described by Longstaffe et al.[4] 128000 scans were used for PFOA and 46080 scans were used for PFP with 128 dummy scans for each, 4096 time domain points, and a recycle delay of 5 x T_1. 0.0001W of saturation power was delivered to ^{19}F nuclei that were found to bind strongest in the ^{19}F observe STD. This was -38923Hz in PFOA and -77895Hz for PFP. Off resonance pulses were +1000000Hz away. Spectra were zero filled by a factor of 2 and processed using an exponential function corresponding to a line broadening of 10Hz in the final spectrum. Reference spectra were acquired with the same conditions except with 1024 scans and 8 dummy scans.

S.2 Demonstration of the Soil Swelling Potential of Pentafluorophenol (PFP) vs. Perfluorooctanoic Acid (PFOA)

Figure S1 illustrates the influence of PFP compared to PFOA. The experiment highlights the components at the soil interface.[5] Figure S1a is a control spectrum of soil swollen without the addition of contaminant and was performed with more scans than Figures S1b and S1c. Figures S1b and S1c were collected with the same number of scans, so the signal to noise (S/N) ratio can be compared in this case. In the case of PFOA the S/N is realtively low, and this along with the generally similar profile to the control indicates the soil is not extensively swollen by PFOA. The main difference to the control is the reduced carbohydrates. This has been previously documented and is seen when the pH of the sample is decreased which in turn makes the carbohydrates more dense and less accessible to water.[6] While the pH of the PFOA

was neutralized prior to addition, it is likely exchange within the soil or concentration of PFOA at the interface may lower the pH locally prevent swelling of the soil organic matter and reduces the accessiblity of the carbohydrates to the aqueous solvent. Conversely, PFP has a considerable affect on the soil-water interface. The S/N is much higher indicating more components are swollen in general. Interestingly some aromatic groups are exposed. Such groups are normally not available at the soil-water interface and are known to be buried under the surface in hydropohobic domains.[5] The swelling of the aromatic and aliphatic components, both considered the most hydrophobic in soil, indicate the liquid PFP bahaves like a solvent and can penetrate into hydrophobic domains. This is interesting as it demonstrates that in the case of a spill it is not the properties of the contaminant or soil alone that will determine contaminant uptake, but that specific physical action of the contaminant itself on the soil may also play a key role in some cases. The ability of CMP-NMR to monitor all aspects of the soil provides a unique window to study such subtle processes.

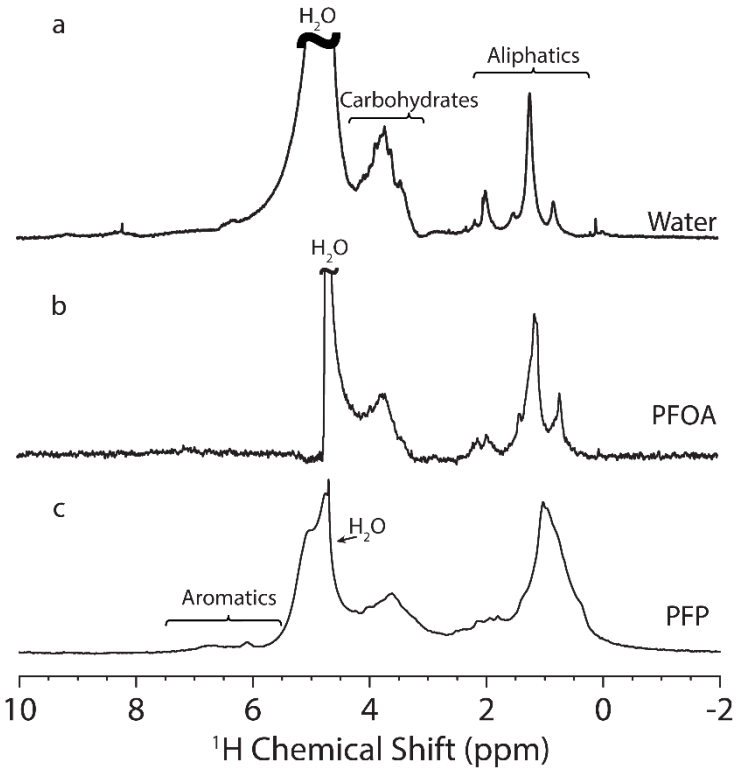

Figure S1: Comparing the influence of different solvents on soil including (a) water, (b) PFOA, and (c) PFP. PFOA has some influence on the aliphatic portion of the soil spectrum while PFP has considerable influence over the entire soil spectrum. Notably, PFP is efficient at swelling the solvent as can be seen through the broadness of the peaks as well as the reduced noise in the spectrum compared to PFOA.

S.3 Spectra for Epitope Map Calculations

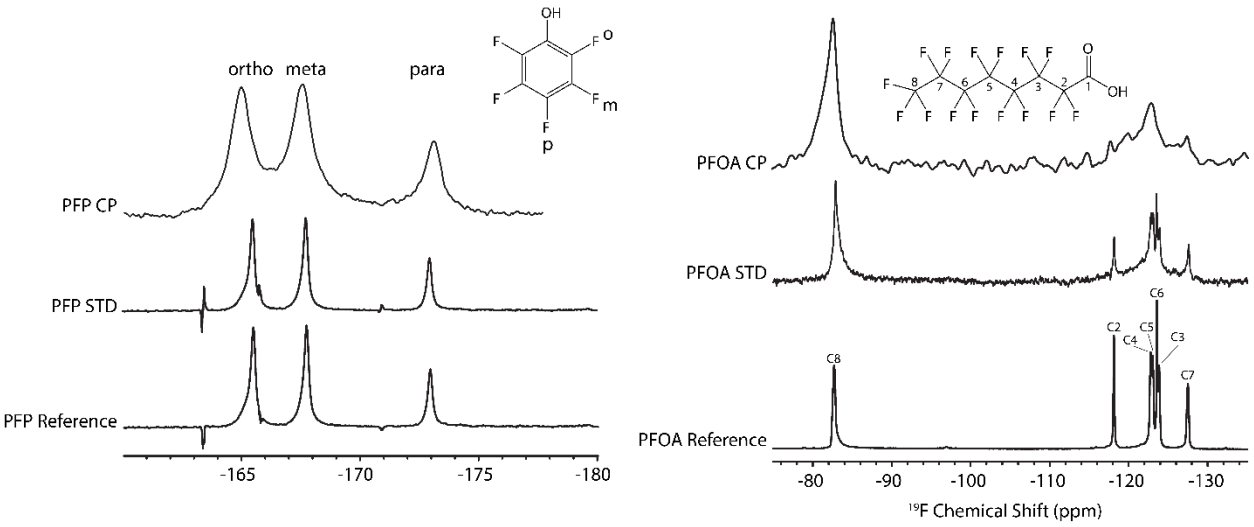

Figure S2: PFP and PFOA reference, STD, and CP spectra used to calculate epitope maps in Figure 2. Note in the case of PFOA CP it is not possible to resolve interactions for CF_2 groups due to low signal to noise. As such, only an average for the entire methylene portion of the chain can be provided (see Figure 3 main manuscript).

S.4 CP Build Up Curve Explanation

CP build up curves were created by monitoring intensity of individual peaks of the contaminants in the ^{19}F spectra as contact time, a CP parameter, is increased. When plotted and fitted according to Equation 1, the result are curves such as those illustrated in Figure 3.

Equation 1:
$$I(t) = \frac{I_o}{1-\frac{T_{HF}}{T_{1\rho}}}\left(e^{-t/T_{1\rho}^{H}} - e^{-t/T_{HF}}\right)$$

CP efficiency is dependent on two variables, the strength of the dipole between two heteronuclei and the relaxation pathways that exist in a spin system. The first variable is represented by T_{HF} in Equation 1. It dictates how fast the curve is built up. The second variable is determined by $T_{1\rho}$, or the relaxation rate constant relative to the rotating frame. The shorter the relaxation time, the quicker the curve will decay.

From this equation, extracting the $1/T_{HF}$ constants from each curve and comparing each provides information of the relative strength of the interaction that exists. Because this can be done for individual peaks of the contaminant, CP build up curve data are another means to test the dynamics in the solid state and to assess the relative strength of binding each position within the molecule.

For PFP the $1/T_{HF}$ values were in agreement with what was found with the CP epitope map (Table S1 and Figure S3). The para fluorine had a largest $1/T_{HF}$ value which translates to a larger dipole strength and therefore contributes the most to PFP binding in soil relative to the other fluorine positions. The meta position had a slightly weaker dipole while the ortho position, closest to the OH group, had the weakest dipole strength. The PFOA build up curve data also followed the same trend that was observed with the CP epitope map. The CF_3 group had a stronger dipole compared to the CF_2 groups. Therefore, the CF_3 group is interacting the strongest with the soil and is responsible for contaminant sequestration while the CF_2 groups contribute relatively less to PFOA sorption in soil.

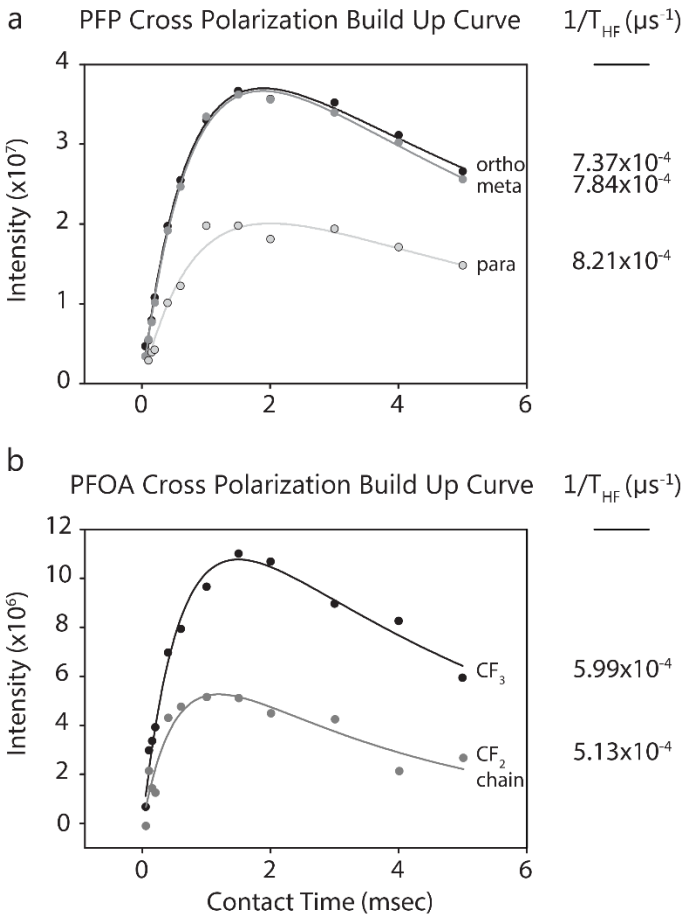

Figure S3: After plotting intensity with contact time and fitting with Equation 1, ^{1}H-^{19}F CP build up curves are formed and $1/T_{HF}$ constants can be extracted which describe the strength of interaction between different functional groups from the contaminants and soil. The results support the findings in the solid state epitope maps suggesting that the ^{19}F in the para position contributes the most to PFP sequestration while the CF_3 is responsible for binding in PFOA.

Table S1: List of T_{HF} values and errors calculated from plotting CP build up curves using Equation 1

	T_{HF} (µs)	Error	$1/T_{HF}$ (μs^{-1})
PFOA CF_3	1668.671	210.2461	5.99E-04
PFOA CF_2 Chain	1947.775	614.2192	5.13E-04
PFP ortho	1357.25	95.7044	7.37E-04
PFP meta	1276.245	77.7812	7.84E-04
PFP para	1217.832	273.734	8.21E-04

S.5 Further Considerations

CMP-NMR is a versatile tool to follow complex processes in complex environmental media. Its ability to analyze individual physical states provides two important opportunities: 1) Separating physical states spectroscopically allows the user to study complex media without chemical or physical treatment thus maintaining the natural state and important facets such as the aqueous interface, the biologically active state, and native conformation and, 2) provides unprecedented molecular detail and experimental versatility to extract novel molecular information that is hard or impossible to decipher using more conventional approaches. CMP-NMR has a wide variety of uses and great potential in environmental research and other fields. The major drawback of CMP-NMR is its relatively low sensitivity. In large part this arises not from the probes themselves but studying samples in their native state. Consider for example if natural soil is 50% water. Then a researcher aims to study ^{13}C in solid components only in a

swollen sample. If it is argued that only 50% of the organic matter is truly solid then the signal from the solid-state in the native state is only ~25% when compared to a conventional solid-state NMR study that packs the sample dry.

Methods to overcome this problem revolve around further advancement of NMR technology including the development of CMP-NMR cryoprobes and dynamic nuclear polarization.[7, 8, 9] However the simplest solution may be the development of larger diameter probes that simply introduce more sample. In turn this may permit lower ratios of contaminant to soil to be used with an eventual and future transition towards trace contaminant levels.

Perfluorinated contaminants were used here as they are both environmentally relevant, and fortuitously, ^{19}F is an excellent NMR nucleus in terms of both sensitivity and spectral dispersion. However while many potential contaminants (agrochemicals, pharmaceuticals, personal care products) do contain ^{19}F, the majority do not. In many cases other heteronuclei such as ^{15}N, ^{27}Al, ^{29}Si, ^{31}P, ^{51}V, ^{75}As, ^{113}Cd, ^{199}Hg, ^{207}Pb may be naturally present and could be used along with a suitably tuned CMP-NMR probe. In the case of organic contaminants one solution may be to isotopically label contaminants with ^{2}H. ^{2}H can replace ^{1}H without significantly altering the chemical properties of a compound permitting a wide range of contaminants to be studied albeit with lower sensitivity afforded by ^{2}H NMR.[10, 11] Interestingly, ^{3}H is the most sensitive of all NMR nuclei (more than ^{1}H), but its radioactive nature would require stringent safety protocols and certification that may be out of reach for most multi-user NMR centers. In summary, however, the ability of CMP-NMR to provide unprecedented information on both structure and molecular interactions, for all components in natural

unaltered samples, suggest it has an important and key role in unravelling and explaining complex environmental processes both now and in the future.

REFERENCES

1. Wu, D. H.; Chen, A. D.; Johnson, C. S. An Improved Diffusion-Ordered Spectroscopy Experiment Incorporating Bipolar-Gradient Pulses. *Journal of Magnetic Resonance Series a.* **1995,** *115* (2), 260-264.

2. Courtier-Murias, D.; Farooq, H.; Masoom, H.; Botana, A.; Soong, R.; Longstaffe, J. G.; Simpson, M. J.; Maas, W. E.; Fey, M.; Andrew, B.; Struppe, J.; Hutchins, H.; Krishnamurthy, S.; Kumar, R.; Monette, M.; Stronks, H. J.; Hume, A.; Simpson, A. J. Comprehensive multiphase NMR spectroscopy: Basic experimental approaches to differentiate phases in heterogeneous samples. *J. Magn. Reson.* **2012,** *217* 61-76.

3. Masoom, H.; Courtier-Murias, D.; Farooq, H.; Soong, R.; Simpson, M. J.; Maas, W.; Kumar, R.; Monette, M.; Stronks, H.; Simpson, A. J. Rapid estimation of nuclear magnetic resonance experiment time in low-concentration environmental samples. *Environ. Toxicol. Chem.* **2013,** *32* (1), 129-136.

4. Longstaffe, J. G.; Simpson, A. J. Understanding Solution-State Noncovalent Interactions between Xenobiotics and Natural Organic Matter using F-19/h-1 Heteronuclear Saturation Transfer Difference Nuclear Magnetic Resonance Spectroscopy. *Environ. Toxicol. Chem.* **2011,** *30* (8), 1745-1753.

5. Simpson, A. J.; Kingery, W. L.; Shaw, D. R.; Spraul, M.; Humpfer, E.; Dvortsak, P. The application of H-1 HR-MAS NMR spectroscopy for the study of structures and associations of organic components at the solid - Aqueous interface of a whole soil. *Environ. Sci. Technol.* **2001,** *35* (16), 3321-3325.

6. Farooq, H.; Courtier-Murias, D.; Soong, R.; Bermel, W.; Kingery, W. M.; Simpson, A. J. HR-MAS NMR Spectroscopy: A Practical Guide for Natural Samples. *Curr. Org. Chem.* **2013,** *17* (24), 3013-3031.

7. Bross-Walch, N.; Kühn, T.; Moskau, D.; Zerbe, O. Strategies and tools for structure determination of natural products using modern methods of NMR spectroscopy. *Chemistry and Biodiversity.* **2005,** *2* (2), 147-177.

8. Ardenkjær-Larsen, J. H.; Fridlund, B.; Gram, A.; Hansson, G.; Hansson, L.; Lerche, M. H.; Servin, R.; Thaning, M.; Golman, K. Increase in signal-to-noise ratio of >10,000 times in liquid-state NMR. *Proc. Natl. Acad. Sci. U. S. A.* **2003,** *100* (18), 10158-10163.

9. Maly, T.; Debelouchina, G. T.; Bajaj, V. S.; Hu, K. -.; Joo, C. -.; Mak-Jurkauskas, M. L.; Sirigiri, J. R.; Van Der Wel, P. C. A.; Herzfeld, J.; Temkin, R. J.; Griffin, R. G. Dynamic nuclear polarization at high magnetic fields. *J. Chem. Phys.* **2008,** *128* (5),

10. Zumbulyadis, N.; Landry, C. J. T.; Long, T. E. Determination of Polymer Miscibility by Proton Deuterium CP/MAS NMR-Spectroscopy. *Macromolecules.* **1993,** *26* (10), 2647-2648.

11. Akbey, U.; Camponeschi, F.; van Rossum, B.; Oschkinat, H. Triple Resonance Cross-Polarization for More Sensitive C-13 MAS NMR Spectroscopy of Deuterated Proteins. *ChemPhysChem.* **2011,** *12* (11), 2092-2096.